BASIC ELECTRONIC PROPERTIES OF a-Si:H/c-Si HETEROSTRUCTURE SOLAR CELLS

M. Schmidt[1], L. Korte[1], K. Kliefoth[1], A. Schoepke[1], R. Stangl[1], A. Laades[1], E. Conrad[1] , K. Brendel[1], W. Fuhs[1]
M. Scherff[2], W. Fahrner[2]

[1] Hahn-Meitner-Institut Berlin, Abteilung Silizium-Photovoltaik, Kekuléstr. 5, D-12489 Berlin

Tel: +49/30/8062-1352, Fax: +49/30/8062-1333, e-mail: schmidt-m@hmi.de

[2] University of Hagen, Department of Electrical Engineering Haldener Str. 182, D-58084 Hagen,
Tel.: ++49-(0)2331/987-4012, email: maximilian.scherff@fernuni-hagen.de

ABSTRACT: Amorphous/crystalline silicon heterostructures with 2-10nm thin a-Si:H (i,n,p) layers have been prepared by PECVD deposition and analyzed in respect of their basic properties. The gap state densities of the thin a-Si:H layers have been determined by UV-excited photoelectron spectroscopy. The concentration of deep states depends on the doping level and lies in the range between 10^{18}-10^{20}cm^{-3}. The Fermi level, resulting from UPS analysis, shifts up to 1.47 eV above the valence band at 10000ppm PH_3 addition to SiH_4. At a-Si:H layer thicknesses below 3nm the onset of the photoelectron contribution from the c-Si valence band gave a value of the valence band offset of 450 ±50meV. The interface state density of the a-Si:H/c-Si interface reaches values down to $2x10^{11}$cm^{-2}eV^{-1} at midgap. These results were obtained from field dependent SPV investigations which indicate an excellent passivation of the interface by the a-Si:H network. Finally, using the optimized preparation parameters, we prepared a ITO/a-Si:H(n)/c-Si(p)/BSF hetero solar cell with an efficiency of 17 %.

Keywords: 1:c-Si - 2:a-Si - 3:Heterojunction

1. INTRODUCTION

Heterostructures have some inherent advantages compared to conventional homo pn junctions because they allow to combine the useful properties of two solids. The heterojunction between amorphous hydrogenated silicon and crystalline silicon, a-Si:H/c-Si, represents such a system which can be prepared at temperatures below 300°C, allowing the application on thin low cost silicon wafers or silicon films on glass. The common challenge of the heterostructures results from the fact that the first monolayers of the heterotransition between both solids determine their properties [1] like the interface state density distribution $D_{it}(E)$, the band offsets between the corresponding valence bands ΔE_V and the conduction bands ΔE_C and the band bending $q\varphi_{SO}$ in the crystalline silicon c-Si. These quantities are sketched in Fig. 1.

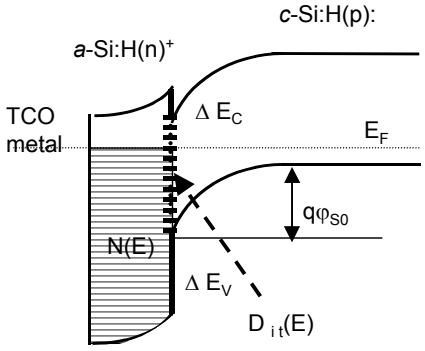

Figure 1: Band scheme of a TCO/a-Si:H/c-Si heterojunction solar cell; interface state density $D_{it}(E)$, gap state density N(E), band offsets ΔE_C and ΔE_V, and band bending $q\varphi_{SO}$.

The aim of this paper is to show how these basic properties influence the solar cell performance, how the quantities can be measured and what their actual values are. This provides the basis for realistic numerical simulations of such heterojunctions by the AFORS-HET programme [2] and for preparation of optimized hetero-solar cells. The potential of this cell type on n-type silicon was demonstrated by the a-Si:H(p)/a-Si:H(i)/c-Si(n) pn-heterojunction solar cell from Sanyo where the cell efficiency η amounts to 17,3% for flat wafers and 20,7% for structured c-Si wafers [3,4].
For the inverse type the Si:H(n)/c-Si(p) np-heterojunction solar cell the reached values amount to η=16.2% on flat c-Si wafers [5], which has been improved up to 17%, as shown in this paper.

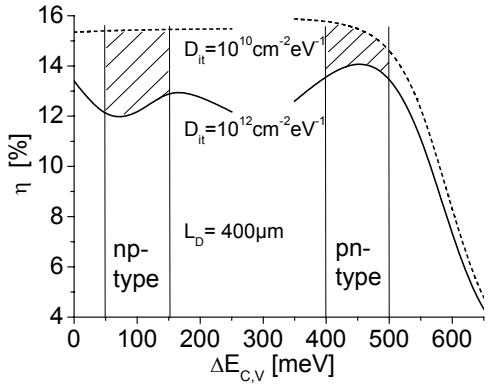

Figure 2: Numerically calculated dependence of the a-Si:H/c-Si hetero solar cell efficiency η on the bandoffset for the minority charge carriers $\Delta E_{C,V}$ for two values of interface state density. The loss in efficiency due to interface recombination is highlighted by the shaded areas for the two cell types.

Fig. 2 makes evident that the most important parameters are the interface state density $D_{it}(E)$ and the bandoffset $\Delta E_{V,C}$ of the minority charge carriers. Their transport across the heterojunction becomes limited at offset values above 450meV. This corresponds to the ΔE_V value of hole transfer at the a-Si:H(p)/c-Si(n) junction. On the other hand, the band offset fixes the Fermi level position directly at the interface and thus determines the interface recombination rate at a given $D_{it}(E)$. The minority band offset for the a-Si:H(n)/c-Si(p) junction goes down to

about $\Delta E_C \approx 100$meV [6] which results in an increased interface recombination at a given $D_{it}(E)$. This emphasizes that the determination of $\Delta E_{C,V}$ and $D_{it}(E)$ are central tasks for physical insights as well as for device development.

2. SAMPLE PREPARATION

All samples were prepared on c-Si substrates (2" or 3"FZ, 1-75 Ωcm) with (111) surface orientation. After cleaning the wafers by the standard RCA process and a HF-dip (1% HF, 60 sec) the substrates were inserted into the CVD deposition chamber within 5 minutes. The passivation of the substrate surface (H-termination) by the HF-dip is known to be stable against oxidation for about 30 minutes [7]. The a-Si:H layers were deposited by plasma enhanced chemical vapor deposition (PECVD) at 13.56 MHz and 15-55 mW/cm^2 power density. Process gases were semiconductor grade silane (SiH_4) phosphine (PH_3) or diboran (B_2H_6) and pure hydrogen. Gas flow, H-dilution and the sample temperature during deposition (170°C...250°C) were varied for layer and interface optimization. Immediately after deposition, the samples were transferred to the photoelectron spectroscopy analysis chamber without breaking the vacuum or were stored in dry nitrogen for SPV measurements. For the preparation of n/p-type heterojunction solar cells we used flat, 350 µm thick, (111) oriented, monocrystalline FZ silicon wafers (0.5 – 2Ωcm) with a diffused back suface field (BSF). After the wafer cleaning, as desribed above, the a-Si:H (n) layer was deposited. After that, an indium tin oxide (ITO) layer with a thickness of 80 nm, an integral transmission of 86 % and a specific resistance of $3x10^{-4}$ Ωcm was deposited by dc-sputtering from a compound target. Finally, the front and back contacts were prepared by thermal evaporation. 30 nm Cr and 3µm Ag layers structured with photolithography are used on the ITO and 2 µm Al (full area) is deposited on the backside. Cells with an area of 1cm^2 are prepared by wet chemical etching the ITO in order to separate the cells.

3. EXPERIMENTAL METHODS

3.1 Photoelectron Spectroscopy (PES)

The energetic distribution of the occupied gap states and upper valence band states $N_{OC}(E)$ and the Fermi level position were determined by UV excited (hν=3-7eV) photoemission. The photoemission yield is determined by the distributions of the occupied and unoccupied states, $N_{OC}(E)$ and $N_U(E)$, and the optical transition matrix element [8]. Assuming a constant density of states (DOS) of the unoccupied final states $N_U(E)$ [9] and assuming that the optical matrix element remains nearly constant up to hν= 3.5 eV and decreases above this value as shown in [8], the measured yield Y(E), corrected by the optical matrix element, directly traces $N_{OC}(E)$.

For excitation energies below 10eV the inelastic mean free path, λ_{imfp}, of the photoelectrons, depending on the interaction with phonons, electrons and plasmons, strongly raises up to about 5nm at 6eV because energy losses by plasmon generation processes are impossible [10]. The detection limit of the electron emission depth can be assumed to be about $3\lambda_{imfp}$. Therefore, excitation in the energy range between the work function limit at 3.8eV and about 7eV allows the measurement of the DOS of ultrathin a-Si:H layers with a thickness of 5-7nm. The photoelectrons were excited by strong monochromatic UV-light (3–7.5eV) generated by passing the light of a Xe high pressure lamp through a double-grating monochromator. In this low excitation energy range, the number of absorbed photons was measured using calibrated silicon diodes for the detection of the incoming and reflected light beams. This procedure allows to measure the absolute photoelectron quantum yield Y(E) at each photon energy in two different modes. In the first mode, corresponding to standard UPS, the distribution of the kinetic energy of the photoelectrons was detected during excitation with a fixed photon energy. In the other mode, the energy analyzer was operated at a fixed energy (final state energy) while varying the photon energy (3-7eV), a technique known as Constant Final State Yield Spectroscopy (CFSYS). The energy resolution of the analyzer was better than 100meV.

3.2 Surface photovoltage (SPV)

The surface photovoltage method allows to determine both the band bending in the c-Si absorber and the interface state density distribution. For that purpose the change in band bending caused by optically generated charge carriers is monitored and the initial band bending is changed by applying an external voltage. The decay with time of excess charge carriers after their generation in c-Si by a light pulse (λ=934nm, 150ns pulse length) is measured as the voltage decay of an artificial MIS structure. The artificial MIS structure consists of the glas/TCO/mica/a-Si:H/c-Si/Al sample where the top (metal) electrode is a TCO covered glas plate followed by mica as an insulator. The solution of Poisson's equation for the space charge region at the (free) sample surface (c-Si) yields the space charge density of the band bending region $Q_{SC}=\text{const}\cdot F(\varphi_0,\lambda,\delta p)$, where $F(\varphi_0,\lambda,\delta p)$-doping function, φ_0-initial band bending, $\lambda=p/n_i$ - doping factor, δp - excess charge [11].

To determine the initial band bending from the doping function presumes that no recharging during the light pulse takes place, i.e. $F_0(\varphi_0,\lambda,\delta p=0) = F(\varphi,\lambda,\delta p\neq 0)$. This means that during the light exposure (pulse length ~150 ns), no states at the a-Si:H/c-Si interface or close to it change their charge state. In this case the photovoltage is given by the band bending change before and at the end of illumination, corrected by the Dember voltage U_D, which results from the different mobilities of the electrons and holes ; $U_{ph}=(\varphi-\varphi_0)-U_D$. The determination of the interface state density distribution needs the correctly measured band bending φ_S and their relation to the applied external gate voltage U_g. The method for determining $D_{it}(\varphi_S)$ is given in detail in [12].

4. RESULTS AND DISCUSSION

First the UPS and CFSYS modes were used to determine the position of the Fermi level with respect to the valence band edge $E_F - E_V$, the slope of the valence band tail states (Urbach energy E_O) and the variation of the distribution of dangling bond (db) states with doping. The Fermi level position results directly from the zero point of the binding energy E_B. From the slope of the straight line in a plot of √Y(E) vs. E the onset of the

parabolic density of states distribution at the valence band edge is determined which defines the value of E_V. At
this energy the density of states amounts to $N_{OV} \approx 2 \times 10^{21} cm^{-3} eV^{-1}$ [8]. This value was used here to define a quantitative scale for the DOS distribution. The Urbach energy E_{OV} of the exponentially distributed valence band tail states was obtained from the slope of a log-linear plot of $N_{OC}(E)$ vs. E. The obtained value of E_{OV} reflects the disorder broadening of the valence band with doping as shown from curves (1), (2) and (3) in Fig. 3. The E_{OV} amounts to 91meV, 136meV and 120meV, respectively. These are ordinary values for doped a-Si:H layers [9]. Additionally, it can be seen that the deep defect state density decreases for slightly doped compared to the n-doped layers by nearly one order of magnitude. The deep defect density of curve (3) is not measurable because only occupied states can be detected by PES according to $N(E)_{OC}=N(E)\cdot f(E)$, where f(E) is the Fermi-Dirac distribution function.

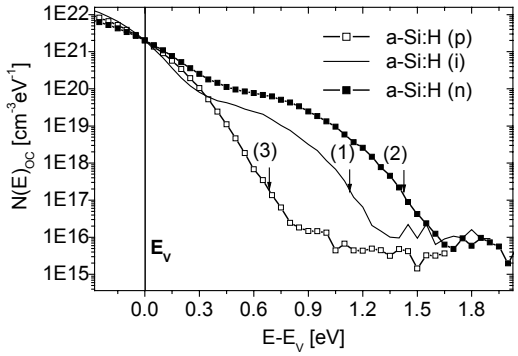

Figure 3: Gap state density distribution $N_{OC}(E)$ derived from CFSYS of a-Si:H(i) non intentionally doped (1), a-Si:H(n) doped with $2x10^4$ ppm PH_3 (2), and a-Si:H(p) doped with 10^4 ppm B_2H_6 (3). PECVD-deposition at 180°C, film thickness 10nm. The arrows mark the position of the Fermi level.

The position of the Fermi level saturates at 1.47eV above E_V by addition of 10^4 ppm PH_3 during the PECVD deposition[13]. This correlates well with E_C-E_F=0.30eV resulting from conductivity measurements at 100nm thick n-doped a-Si:H layers which show a band gap value of 1.75 ±0.05eV [13, 14].

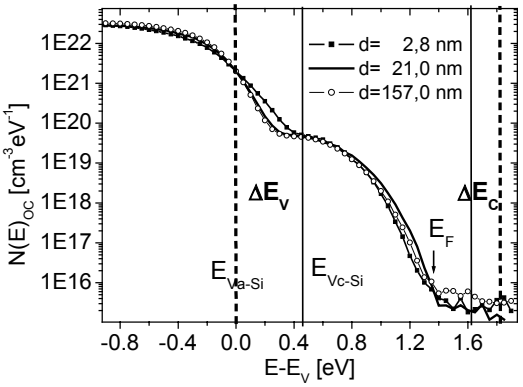

Figure 4: $N_{OC}(E)$ of slightly n-doped a-Si:H of different film thickness prepared by PECVD on c-Si((p),(111), 75Ωcm). The data result from constant final state yield measurements, the chosen final state energy amounts to 200meV. Excitation energy range hν=4...7eV. The arrow indicates the Fermi level position $(E_F - E_{Va\text{-}Si}) = 1.33$eV and the dashed lines indicate the position of the band edges of a-Si:H and the solid lines the c-Si band edges, respectively.

The basic characteristics of the gap state distribution are nearly unchanged when the layer thickness is reduced to values down to 2.8 nm (Fig. 4). This was confirmed by measurements on different series of samples deposited with varying thickness on c-Si (111), c-Si (100) and also on Ag-coated wafers. It is surprising that the density of deep defects changes only very little even in the thinnest sample. However, there is clearly a change of the slope of the valence band tail. E_{OV} increases from 73meV for the thick layers to 101meV for the ultrathin layer (2.8nm) (Fig.4). Based on the comparison with $N_{OC}(E)$ spectra of 2nm thin a-Si:H on an Ag substrate we believe that this results from contributions of the crystalline silicon substrate to the photoemission. A measurable contribution of photoelectrons from the c-Si substrate can be expected only for a-Si:H layer thickness d<5nm due to the small value of the electron emission depth. This condition is fulfilled for the thinnest layer and the contribution from the occupied states of the silicon valence band gives a direct measure of the valence band offset at the interface between a-Si:H and c-Si, which yields ΔE_V=450±50meV. This is in agreement with CFSYS results [6] and compatible with the 100meV conduction band offset as we measured independently by internal photoemission.

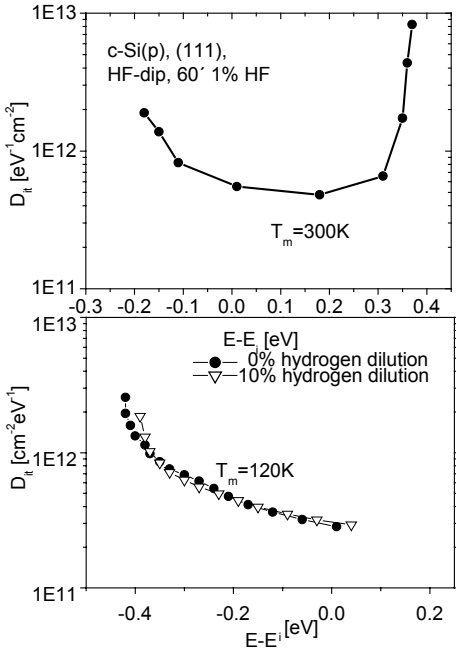

Figure 5a,b: (a) Interface state density distribution $D_{it}(E)$ at the c-Si(p, (111)) surface after H-termination by 1min HF-dip in 1% HF:H_2O. Measured by SPV at room temperature.
(b) Interface state density distribution $D_{it}(E)$ at the a-Si(i):H/c-Si(p,(100)) hetero interface measured by SPV at 120K. The a-Si:H(i) thickness amounts to 8nm, deposited at 230°C by PECVD with different H-dilution of silane.

The interface state density distribution $D_{it}(E)$ after wafer cleaning and H termination of the c-Si surface is very important because the c-Si surface becomes an active part of the hetero interface. The growth of silicon oxide after the HF dip has to be prevented. An oxide would lead to an increase of the interface state density. $D_{it}(E)$ in Fig5(a) correlates with the number of the non hydrogen-saturated silicon dangling bonds at the c-Si surface [7]. After a-Si:H(i) deposition the interface state density at midgap is further reduced to $D_{it}(E) \approx 2x10^{11}cm^{-2}eV^{-1}$. Such SPV measurements have to be realized at deep temperatures to prevent or minimize the charging of the a-Si:H states near the interface by phonon assisted processes. Therefore, we are only able to reload $D_{it}(E)$ with majority charge carriers. A detailed analysis of the influence of recharge processes during the field dependent SPV measurement reveals that the value of $D_{it}(E)$ measured at deep temperature represents by all means an upper limit. The interface state density below $\approx 2x10^{11}cm^{-2}eV^{-1}$ combined with a band offset of $\Delta E_C \approx 100$ meV gives the opportunity for high efficient hetero solar cells of the type a-Si:H(n)/c-Si(p) as calculated in Fig.2. With an optimized set of preparation parameters we realized solar cells with efficiencies between 16-17% on flat silicon wafers without any high-tech features. The I-V characteristic of the solar cell with 5nm a-Si:H(n)/ 3nm a-Si:H(i) emitter on c-Si(FZ(111), 1Ωcm, p-type) is displayed in Fig. 6.

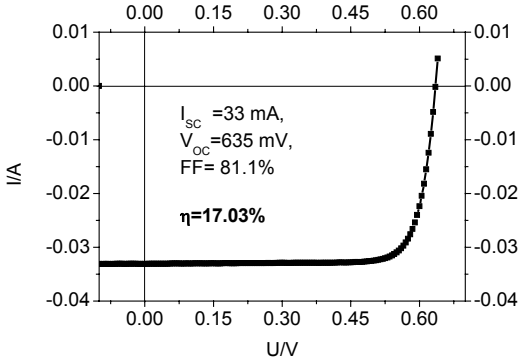

Figure 6: Current Voltage characteristic of the Ag/Cr grid ITO/a-Si:H(n)/a-Si:H(i)/c-Si(p)/BSF/Al hetero-junction solar cell under illumination.

The incorporated thin a-Si(i) layer slightly improves the open circuit voltage up to 635meV and the efficiency by about 0.2%. This effect can be attributed to the reduced defect concentration in the a-Si:H(i) as shown in Fig. 3. This correlates with the numerical simulations in [14, 15] and shows that the efficiency limit for this cell type has been reached and that further improvements mainly depend on the minority diffusion length in the c-Si(p) wafer.

5. CONCLUSION

The key parameters of TCO/a-Si:H/c-Si hetero-structure solar cells are the recombination active interface states, the band offsets and thus, the Fermi level position at the interface and the built-in band bending in the c-Si. To investigate these quantities we established the surface photovoltage (SPV) method and UV-excited photoelectron spectroscopy (UV-PES). With the help of our numerical simulation programme ARFORS-HET [2] it is possible to check the relevance of the physical quantities for cell efficiency. The n/p type cell is more influenced by the recombination via interface states because of the low minority band offset which leads to a near midgap position of the Fermi level at the interface. Therefore, values of $D_{it}<5\cdot10^{11}cm^{-2}eV^{-1}$ are a precondition for efficient n/p hetero solar cells. This seems fulfilled because of the good dangling bond saturation of the c-Si by the flexible hydrogen-silicon network of the a-Si:H. The valence band offset of 450±50meV determined in a very direct way by UV-PES marks the tolerable limit for a-Si:H(p) emitters on c-Si(n) but does not restrict the function as BSF layer on c-Si(p) absorbers. The direct determination of the Fermi level position in such extremely thin (5-8nm) a-Si:H(n,p) emitter layers by UV-PES is very helpful for optimization of doping. In combination with the band bending measured by SPV we have a complete set of experimentally determined parameters for the description and optimisation of TCO/a-Si:H(n)/c-Si(p)/BSF solar cells. On this basis we can expect efficiencies of 16-17% depending on substrate quality only.

We present such an a-Si:H(n)/c-Si(p) cell with an efficiency of 17% without surface texturing or other high-tech features. This leads us to an optimistic outlook for applying this low temperature solar cell preparation concept on low cost and/or thin film silicon materials.

ACKNOWLEDGEMENTS

This work was supported by the Bundesministerium für Bildung und Forschung (FKZ 01F0012-19) which allowed the realization of a network project concerning the silicon based heterojunction solar cells.

REFERENCES

[1] W.Mönch; Semicond. Surfaces and Interfaces 3rd.Ed. (Springer Berlin)
[2] A. Froitzheim, R. Stangl, M. Kriegel, L. Elstner, W. Fuhs; Proc. WCPEC-3, 3rd World Conference on Photovoltaic Energy Conversion, Osaka, Japan, May 2003, 1P-D3-34
[3] M. Tanaka, M. Taguchi, T. Matsuyama, T. Sawada, S. Tsuda, S. Nakano, H. Hanafusa, Y. Kuwano; Jpn. J. Appl. Phys. **31**(1992)3518.
[4] H. Sakata, T. Nakai, T. Baba, M. Taguchi, S. Tsuge, K. Uchihashi, S. Kiyama; Proc 20th IEEE PVSEC (2000) 7.
[5] M. Scherff, A. Froitzheim, A. Uljaschin, M. Schmidt, W. Fuhs, W.R. Fahrner; Proc. PV in Europe Conf., Rom, Italy, Oct.2002,123-126
[6] C. Bittencourt, F. Alvarez, in *Properties of amorphous silicon and its alloys,* T. Searle, EMIS Data-Review Series No. 19, 1998.
[7] H. Angermann, W. Henrion, M. Rebien, A. Röseler Solar Energy Mat. and Solar Cells 83/4 (2004) 331
[8] W. B. Jackson, S.M. Kelso, C.C. Tsai, J.W. Alien, S.-J- Oh; Phys. Rev. **B31** (1985) 5187
[9] K. Winer, L. Ley; Phys. Rev. **B36** (1987) 6072
[10] D.P. Woodruff, T.A. Delchar; Modern techniques of surface science, Cambridge 1992, p.77
[11] C.G.B. Garrett, W.H. Brattain; Phys. Rev. **99**, 2 (1955) 376
[12] Y.W. Lam; J. Phys. D: Appl.Phys. **4** (1971) 1370
[13] M. Schmidt, A. Schöpke, O. Milch, T. Lussky, W. Fuhs; Mat. Res. Symp.Proc. **762** (2003) A19.11.1
[14] Froitzheim, PhD thesis 2003, Universität Marburg, Germany
[15] R. Stangl, A. Froitzheim, M. Schmidt, W. Fuhs Proc. WCPEC-3, 3rd World Conf. on Photovoltaic Energy Conversion, Osaka, Jpn, 05(2003)4P-A8-45